# Radiomic Signature as a Predictive Factor for Lymph Node Metastasis in Early-Stage Cervical Cancer

Yangyang Kan, MD,[1,2,3] Di Dong, MD,[4,5] Yuchen Zhang, MS,[6] Wenyan Jiang, MD,[2,3] Nannan Zhao, MD,[2,3] Lu Han, MM,[2,3] Mengjie Fang, MS,[4,5] Yali Zang, MD,[4,5] Chaoen Hu, MD, MD,[4,5] Jie Tian, MD,[4,5]* Chunming Li, MD,[6]* and Yahong Luo, MD[1,2,3]*

**Background:** Lymph node metastasis (LNM) is the principal risk factor for poor outcomes in early-stage cervical cancer. Radiomics may offer a noninvasive way for predicting the stage of LNM.
**Purpose:** To evaluate a radiomic signature of LN involvement based on sagittal $T_1$ contrast-enhanced (CE) and $T_2$ MRI sequences.
**Study Type:** Retrospective.
**Population:** In all, 143 patients were randomly divided into two primary and validation cohorts with 100 patients in the primary cohort and 43 patients in the validation cohort.
**Field Strength/Sequence:** $T_1$ CE and $T_2$ MRI sequences at 3T.
**Assessment:** The gold standard of LN status was based on histologic results. A radiologist with 10 years of experience used the ITK-SNAP software for 3D manual segmentation. A senior radiologist with 15 years of experience validated all segmentations. The area under the receiver operating characteristics curve (ROC AUC), classification accuracy, sensitivity, and specificity were used between LNM and non-LNM groups.
**Statistical Tests:** A total of 970 radiomic features and seven clinical characteristics were extracted. Minimum redundancy / maximum relevance and support vector machine algorithms were applied to select features and construct a radiomic signature. The Mann–Whitney *U*-test and the chi-square test were used to test the performance of clinical characteristics and potential prognostic outcomes. The results were used to assess the quantitative discrimination performance of the SVM-based radiomic signature.
**Results:** The radiomic signatures allowed good discrimination between LNM and non-LNM groups. The ROC AUC was 0.753 (95% confidence interval [CI], 0.656–0.850) in the primary cohort and 0.754 (95% CI, 0584–0.924) in the validation cohort.
**Data Conclusions:** A multiple-sequence MRI radiomic signature can be used as a noninvasive biomarker for preoperative assessment of LN status and potentially influence the therapeutic decision-making in early-stage cervical cancer patients.
**Level of Evidence:** 3
**Technical Efficacy:** Stage 2

**J. MAGN. RESON. IMAGING 2019;49:304–310.**

View this article online at wileyonlinelibrary.com. DOI: 10.1002/jmri.26209

Received Mar 8, 2018, Accepted for publication May 12, 2018.

The first three authors contributed equally to this work.

*Address reprint requests to: Y.L. Department of Liaoning Cancer Hospital & Institute, No 44, Xiaoheyan Road, Shenyang, 110042, China. E-mail: Luoyahong8888@hotmail.com or C.L., Department of University of Electronic Science and Technology of China, Chengdu, Sichuan, China. E-mail: li_chunming@hotmail.com or J.T., Department of CAS Key Laboratory of Molecular Imaging, Institute of Automation, Chinese Academy of Sciences, No 95, Zhongguancun East Road, Beijing 100190, China. E-mail: jie.tian@ia.ac.cn

From the [1]Dalian Medical University, Dalian, P.R. China; [2]Cancer Hospital of China Medical University, Shenyang, P.R. China; [3]Liaoning Cancer Hospital & Institute, Shenyang, P.R. China; [4]CAS Key Laboratory of Molecular Imaging, Institute of Automation, Chinese Academy of Sciences, Beijing, P.R. China; [5]University of Chinese Academy of Sciences, Beijing, P.R. China; and [6]University of Electronic Science and Technology of China, Chengdu, Sichuan, P.R. China

Additional supporting information may be found in the online version of this article.

 

UTERINE CERVICAL CARCINOMA is one of the most common malignancies and an important cause of cancer-related death among women.[1] Therapeutic alternatives, such as surgery and (chemo) radiotherapy, are currently based on the International Federation of Gynecology and Obstetrics (FIGO) stage of the disease as well as the lymph node (LN) status.[2] LN metastasis (LNM) is the most important independent risk factor for recurrence and death .[3,4,21] While patients with early-stage cervical cancer show a high 5-year survival rate, LNM appearance usually foreshadows sudden, rapid deterioration.[5] Hence, adjuvant chemoradiation is recommended in cases of pelvic LNM diagnosed pathologically after surgery, even if the tumor stage remains unchanged.[1]

Undiagnosed or inaccurately assessed LNMs are a major cause of suboptimal treatment.[6] The standard for LNM diagnosis is histopathologic examination after surgical lymphadenectomy (via laparoscopy). However, the invasive and expensive procedure is not routine and carries a high risk of both short- and long-term complications such as prolonged surgery, blood loss, infection, nerve or vascular injury, lymphocyst formation, venous thromboembolism, and lower extremity lymphedema.[7–10] Therefore, an accurate noninvasive technique for LN status assessment is urgently needed.

Imaging is routinely used for diagnosis, localization, staging, and prognostication. However, the conventional magnetic resonance imaging (MRI) model of diagnosis is based on morphology and size, which cannot reflect the true status of LN.[11,12] Therefore, the identification of more accurate biomarkers for LN status would be valuable for pelvic LNM evaluation before cervical cancer surgery.

Imaging plays a central role in the development of precision medicine.[13] Radiomics, providing more detailed information to describe tumors using vast imaging features extracted from quantitative medical images, has recently become more in vogue.[14,15] The goal of the present study was to preoperatively assess the LNM status in patients with cervical cancer using MRI radiomics.

## Materials and Methods

### Patients

A total of 177 patients (age range, 27–70) with histopathologically confirmed cervical carcinoma clinically staged as FIGO Ia2–IIb underwent MRI examination before biopsy and surgical treatment from March 2014 to October 2017. The patients were scheduled for systematic pelvic lymphadenectomy at our institution, with the gold standard of histologic results available within 2 weeks after MRI. Thirty patients were excluded (Fig. 1) due to some causes.

A total of 143 consecutive patients (mean age, 50; range, 27–70) who met the selection criteria were randomly divided into two cohorts. One hundred patients were allocated to a primary cohort (mean age ± SD, 50.5 ± 9.5; range, 28–70), while 43 patients were allocated to an independent validation cohort (mean age ± SD, 49.9 ± 8.6; range, 27–64). According to histologic results, the primary cohort contained 44 LNM patients and 56 non-LNM patients, and the validation cohort included 14 LNM patients and 29 non-LNM patients. The study was approved by our Institutional Review Board and informed consent was acquired from all patients.

### Clinical and Pathologic Characteristics

Baseline clinical and pathologic characteristics were retrieved from the patient records after obtaining informed consent. Clinical characteristics included age, age of first sexual intercourse, menstrual status, family history of cancer, and pregnancy, parturition, and abortion numbers. Pathologic characteristics included the status of LN.

### MRI Protocols

All patients received MRI examinations before surgery. The MRI images were obtained on a clinical whole-body 3.0T scanner (Siemens Magnetom Verioio, Erlangen, Germany) with a phased-array 8-channel sensitivity encoding abdominal coil. The imaging protocols for MRI are shown in Table 1. The patients drank water to fill the bladder moderately before examination, placed in a supine position, and rested for 15–30 minutes to maintain stable breathing to minimize interference caused by respiratory movement. The scan range covered the entire pelvis. The MRI parameters and body position were the same for all patients.

### Image Analysis

A radiologist with 10 years of experience and a radiologist with 15 years of experience evaluated the images on PACS work station of two sequences. When the evaluation came to a divergence, another senior radiologist assessed the evaluation. They were all blind to clinical data or FIGO stage. The following criteria were assessed for evaluation of nodal metastasis: consideration of size (diameter of the long axis diameter more than 10 mm), shape (round), and border (lobulated or spiculated). The region of LN included bilateral external iliac arteries, obturator arteries, and common iliac arteries. Every region was considered in the LN status.

### Segmentation

We used sagittal $T_1$-enhanced and $T_2$ MRI Digital Imaging and Communications in Medicine (DICOM) original images archived in the Picture Archiving and Communication System (PACS) (Neusoft, Shenyang, China, v. 5.5.5.70228). The segmentation of a region of interest (ROI) is essential for the extraction of quantitative radiomic features. A radiologist with 10 years of experience used the ITK-SNAP open-source software (www.itk-snap.org) for 3D manual segmentation of the primary tumor. A senior radiologist with 15 years of experience validated all segmentations. The ROI covered the whole tumor and was delineated with two sequences (sagittal $T_1$ enhanced and $T_2$ MRI) on each slice.

### Radiomic Feature Extraction and Selection

Image intensity normalization was performed to transform arbitrary MRI intensity values into a standardized intensity range. In all,

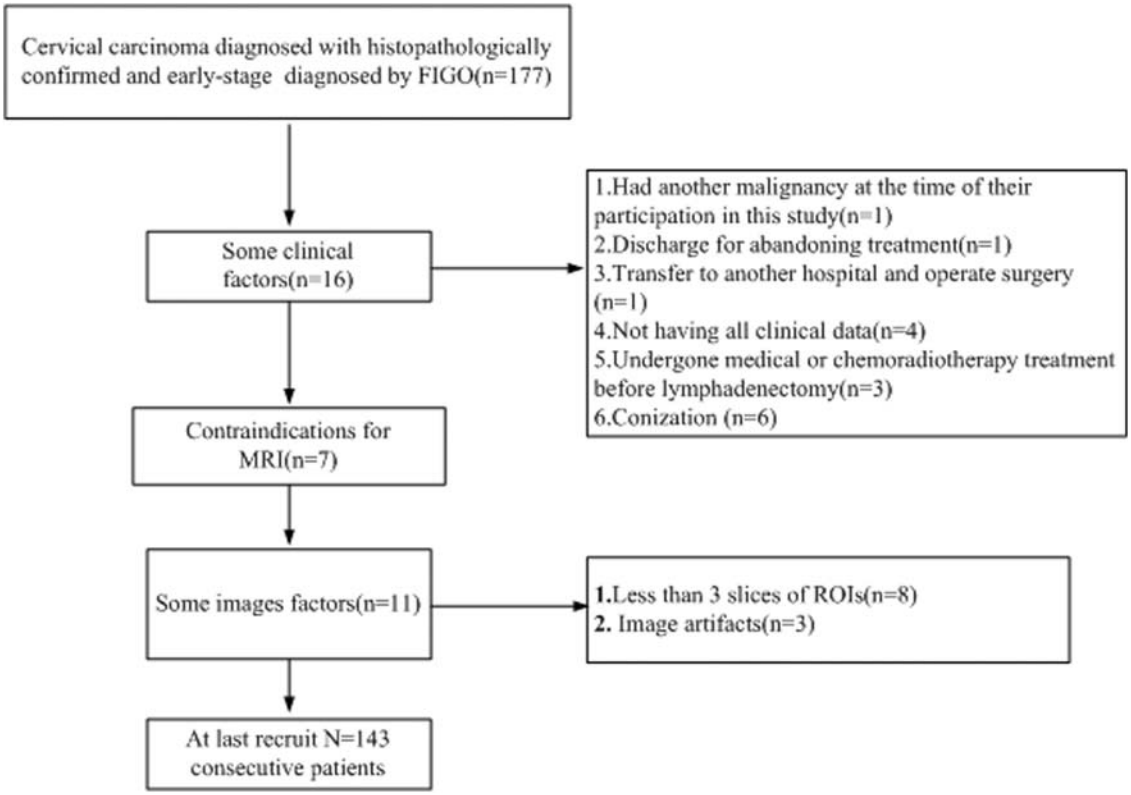


**FIGURE 1: Flowchart of the exclusion criteria.**

485 quantitative radiomic features were calculated from the standard inputs for each sequence. The features were divided into four groups: (I) tumor intensity, (II) shape and size, (III) texture, and (IV) wavelet characteristics (Fig. 2). Their extraction was performed in MatLab 2015b (MathWorks, Natick, MA). A two-step feature selection methodology was applied to the primary cohort. First, the intraclass correlation coefficient (ICC) features, based on 25 randomly chosen images, were calculated to estimate feature robustness. Features with an ICC higher than 0.8 were reserved for each sequence. Second, the minimum redundancy-maximum relevance (MRMR)[16] feature selection algorithm was used to rank all stable features in relation to the LN status. Features mutually far away from each other could still have a high correlation with the LN status. Finally, we used a support vector machine (SVM) algorithm for radiomic signature modeling, and a radiomic signature was calculated based on the SVM model. The distance to the nearest primary data of any class (separation) was maximized by training a hyperplane.

**TABLE 1. MRI Protocols**

| Sequences<br>Parameters | Sagittal T2 | Axial T1 | DCE-MRI | CE T1 |
|---|---|---|---|---|
| TR (msec) | 3800 | 550 | 5.08 | 3.1 |
| TE (msec) | 26 | 13 | 1.74 | 1.25 |
| Slice thickness (mm) | 4 | 4 | | 4 |
| Acquisition matrix | 320x320 | 320x320 | | 202x384 |
| FOV(mm) | 448x396 | 400x400 | | 400x400 |
| Interslice gap | 1 | 1 | | |
| NSA | 2 | 2 | | 2 |
| Contrast agent | | Gd-DTPA | | Gd-DTPA |
| Flip angle | | | 15 | |

FOV, field of view; NSA, number of signals averaged; DCE, dynamic contrast-enhanced; Gd-DTPA, gadolinium diethylenetriaminepentacetate acid (administered as a fast bolus injection in a total dose of 0.1 mmol/kg bodyweight, at a rate of 3mL/s, followed by a saline solution flush (20 mL)).

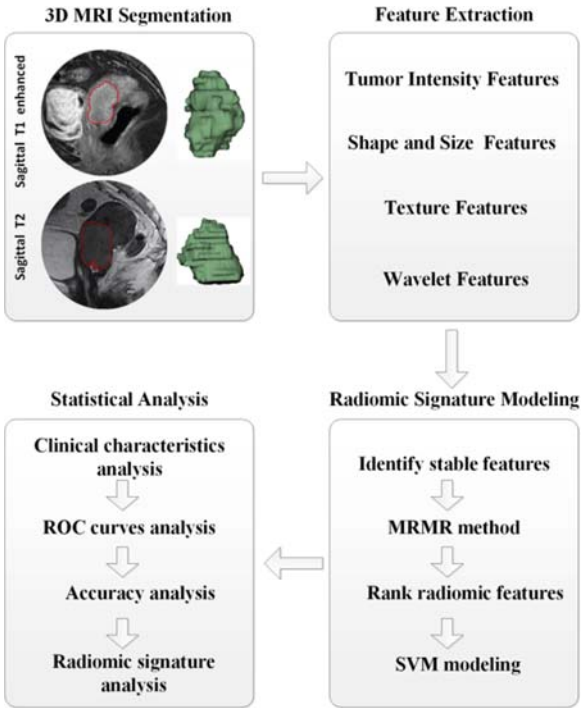


FIGURE 2: Workflow of this study.

### *Statistical Analysis*

We analyzed the accuracy, sensitivity, and specificity of assessment of metastatic node based on MRI images by radiologists with SPSS v. 19.0 (Chicago, IL). In univariate analysis, the Mann–Whitney *U*-test and the chi-square test were used for continuous and categorical variables, respectively, to test the performance of clinical characteristics and potential prognostic outcomes. $P < 0.05$ was considered to indicate statistical significance. The area under the receiver operating characteristics curve (ROC AUC), classification accuracy, sensitivity, and specificity were used to assess the quantitative discrimination performance of the SVM-based radiomic signature in the primary and validation cohorts. The point on the ROC curve with the maximum positive likelihood ratio was considered the optimal cutoff threshold value. These prediction measures were computed using the R package pROC, and MRMR feature selection was done using the MRMRe package. Statistical methods were based on the R analysis platform (Vienna, Austria, v. 3.3.1).

## Results

### *Performance of the Image Analysis*

In the primary cohort, the number of metastatic nodes from MRI accessed by radiologists was 67 of the 100 patients, and the true number of metastatic nodes was 44 of 100. In the validation cohort, the number of metastatic nodes assessed by the radiologist was 28 of the 43 patients, and the true number of metastatic nodes was 14 of 43. The classification accuracy, sensitivity, and specificity of the image analysis in the primary and validation cohorts are shown in Table 2.

### *Clinical Characteristics*

The patients were classified into two groups, LNM and non-LNM, based on the results of histopathology from systematic pelvic lymphadenectomy. The clinical characteristics of all patients, such as age, pregnancy number, and parturition number, are summarized in Table 3. No significant differences in any characteristics ($P > 0.05$) between the LNM and non-LNM groups in both the primary and validation cohorts were found by univariate analysis.

### *Feature Selection and Radiomic Signature Modeling*

The sagittal $T_1$ enhanced and $T_2$ sequences had 176 and 289 stable features, respectively, after the first feature selection step. We applied the MRMR method to the 465 stable features and used the top 10 MRMR-ranked features to train a linear SVM model on the primary cohort. The description of the selected 10 features is presented in the Supplementary Information. The radiomic signature score of each patient was calculated based on the SVM model. The 10 features were ranked based on an MRMR feature selection algorithm as follows: T2sag_1_GLRLM_LRE, T1sagC_0_GLRLM_LRHGLE, T2sag_8_fos_root_mean_square, T1sagC_7_GLCM_sum_average, T1sagC_2_GLRLM_LRE, T1sagC_0_fos_uniformity, T2sag_7_GLCM_variance, T1sagC_1_fos_median, T2sag_1_GLRLM_RP and T1sagC_5_fos_skewness.

### *Radiomic Signature Performance Validation*

The ROC analysis, as well as the distributions of the radiomic signature and LN status in the primary and validation cohorts, is shown in Fig. 3. The radiomic signature showed a satisfactory predictive performance with AUCs of 0.753 (95% confidence interval [CI], 0.656–0.850) in the primary cohort and 0.754 (95% CI, 0584–0.924) in the validation cohort. Moreover, there was a significant association between the radiomic signature and LN status in the primary cohort ($P < 0.01$), which was confirmed in the validation cohort ($P < 0.01$). The classification accuracy, sensitivity, and specificity of the radiomic signature in the primary and validation cohorts are shown in Table 4.

TABLE 2. Performance of the Image Analysis

| Metric | Image analysis | |
|---|---|---|
| | Primary cohort | Validation cohort |
| Accuracy | 0.650 | 0.488 |
| Sensitivity | 0.863 | 0.714 |
| Specificity | 0.482 | 0.379 |

T2

**TABLE 3. Characteristics of Patients in the Primary and Validation Cohorts**

| Characteristic | Primary cohort | | | Validation cohort | | |
|---|---|---|---|---|---|---|
| | LNM group | Non-LNM group | *P* | LNM group | Non-LNM group | *P* |
| Age (Mean ± SD) | 49.11 ± 10.09 | 51.50 ± 8.89 | 0.576 | 51.57 ± 9.22 | 49.10 ± 8.35 | 0.376 |
| Pregnancy no. (mean ± SD) | 3.09 ± 1.51 | 3.13 ± 1.60 | 0.937 | 2.29 ± 1.27 | 2.79 ± 1.47 | 0.280 |
| Parturition no. (mean ± SD) | 2.10 ± 0.85 | 1.80 ± 0.76 | 0.758 | 1.36 ± 0.84 | 1.27 ± 0.83 | 0.431 |
| Abortion no. (mean ± SD) | 1.55 ± 1.37 | 1.59 ± 1.47 | 0.954 | 0.93 ± 1.00 | 1.24 ± 1.18 | 0.454 |
| First age of sexual intercourse (mean ± SD) | 23.55 ± 2.56 | 23.00 ± 4.08 | 0.748 | 22.64 ± 2.62 | 22.93 ± 2.46 | 0.509 |
| Menstrual status | | | 0.927 | | | 0.812 |
| Menstruation, *n* (%) | 16(11.19%) | 22(15.389%) | | 5(3.50%) | 13(9.10%) | |
| Menopause, *n* (%) | 28(19.58%) | 34(23.78%) | | 9(6.29%) | 16(11.19%) | |
| Family history of cancer, *n* (%) | | | 0.975 | | | 0.815 |
| No | 41(28.67%) | 53(37.06%) | | 14(9.79%) | 27(18.88%) | |
| Yes | 3(2.10%) | 3(2.10%) | | 0(23.81%) | 2(1.40%) | |
| Radiomic signature score, median (interquartile range) | 0.482 (−1.543 to 1.223) | −0.104 (−1.575 to 1.217) | <0.001 | 0.602[a] (−0.910 to −1.288) | 0.017 (−1.686 to 1.108) | 0.016[a] |

*P* values were derived from univariate association analyses between each characteristic and clinical status.LNM, lymph node metastasis.
[a]$P < 0.05$.

## Discussion

Radiomic studies of LNM in patients with bladder and rectal cancer have reported satisfactory predictive accuracies.[17,18] These studies used radiomic signatures based on a single category of computer tomography (CT) features. The two-sequence radiomic signature showed a good predictive performance for LN status not only in the primary cohort, but also in the validation cohort.

Radiomics is a rapidly emerging discipline aiming to extract high-throughput quantitative features from digital tomographic images (CT, MRI, or positron emission tomography) that can be converted into mineable high-dimensional data. Radiomic features combined with patient/tumor characteristics can be leveraged via clinical decision support systems to improve medical decision-making, in turn resulting in improved diagnostic, prognostic, and predictive accuracies, as well as facilitating therapeutic research.[19,20] Thus, radiomic signature biomarkers may be helpful in identifying patients who may need LN biopsies.

Knowledge of the LN status is essential to make an informed choice between surgery (radical hysterectomy) and adjuvant treatment.[21] The gold standard for LN status assessment in early-stage cervical cancer is histopathologic examination, which is invasive and expensive, and carries a high risk of complications. In early-stage cervical cancer, the percent of LNM is about 15%, which means that the number of node-negative patients may be as high as 85%. These patients may have no direct benefit from LN dissection.[22–24] One feasible approach to determine the LN status preoperatively is to develop radiomic models using signatures from medical images to evaluate the likelihood of LN involvement. The present study offers a noninvasive and repeatable radiomic prediction tool to identify the LN status in patients with early-stage cervical cancer.

Compared to clinical examination, medical imaging provides more information for patient evaluation and may lead to more appropriate therapeutic decisions. MRI is commonly used to distinguish between metastatic and benign LNs. LNs can be evaluated by MRI based on their size and morphologic aspect. Nodal involvement is indicated by increased size (>1 cm or 0.8 cm), round shape, irregular margins, and other characteristics, such as nodal-inside change and enhanced by contrast agents.[21,25–27] However, these morphologic findings are not sufficient for accurate diagnosis. In addition, MRI cannot discriminate between enlarged inflamed and metastatic LNs. In our study, the accuracy of our method was higher than that assessed by a radiologist, indicating superiority over conventional assessment of metastatic node from MRI by a radiologist.

The risk factors for cervical cancer include age, first age of sexual intercourse, menstrual status, family history of cancer, and pregnancy, parturition, and abortion numbers.[28]

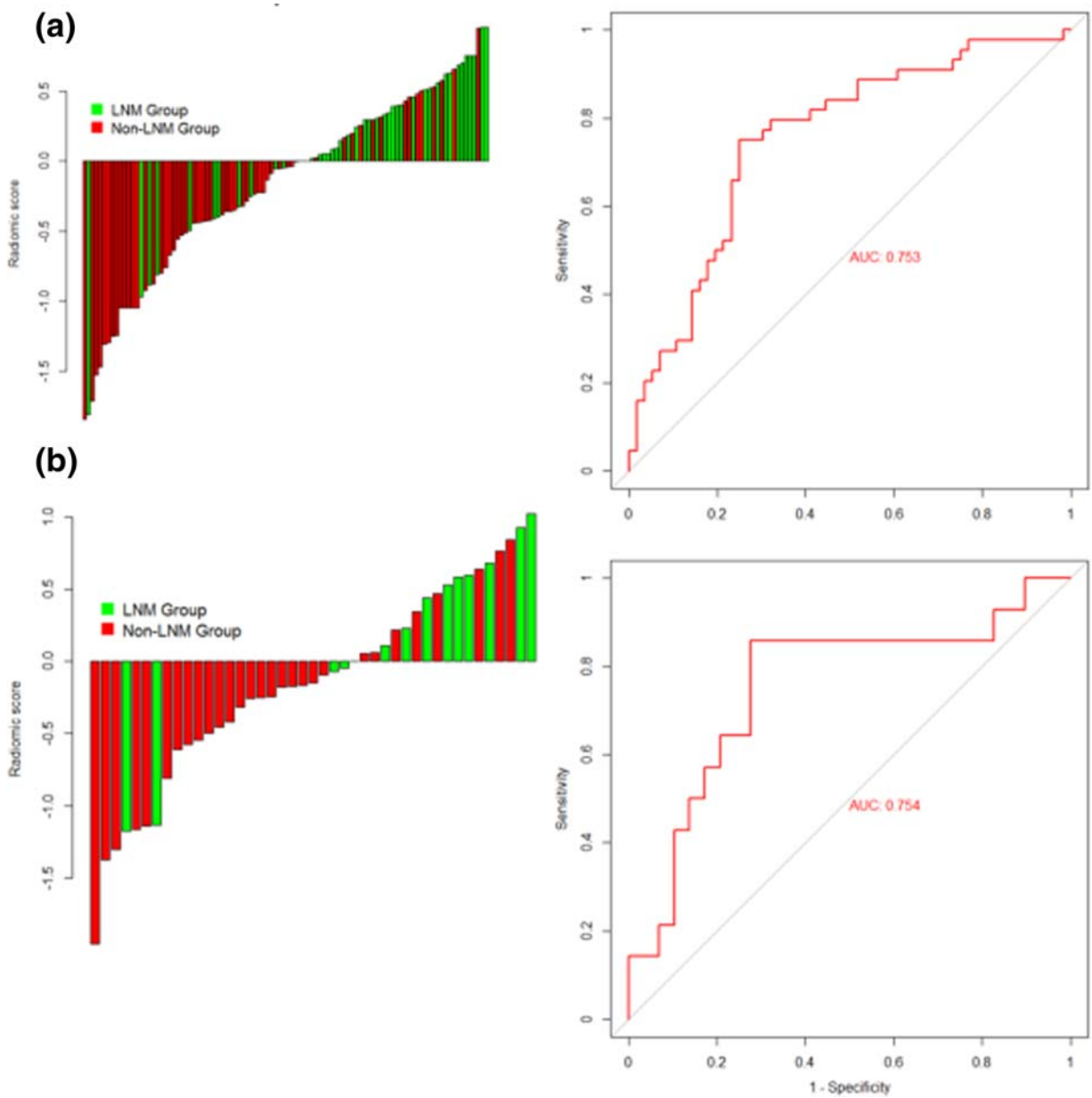


**FIGURE 3: The SVM performance of predicting LN statue. (A) Primary cohort: A radiomic signature score corresponding to each patient; the red marks and green marks indicate the patients in the LNM group and non-LNM group, respectively, and the AUC for the radiomic signature score. (B) Validation cohort: A radiomic signature score corresponding to each patient; the red marks and green marks indicate the patients in the LNM group and non-LNM group, respectively, and the AUC for the radiomic signature score.**

However, we found no statistically significant differences in any of these characteristics between patients with and without LNM in either the primary or validation cohort, which may be caused by a lack of geographic and ethnic diversity in the study population. Larger cohorts need to be studied to validate our findings.

Our study has several limitations. First, all data were obtained from a single research center using one specific type of MR scanner, which may have resulted in a selection bias. Multicenter validation is needed in the future. Second, more recently the LNM number, log odds of positive LNs, and lymph node ratio have been shown to be the strongest

**TABLE 4. Performance of the Radiomic Signature**

| Metric | Radiomic signature | |
|---|---|---|
| | Primary cohort | Validation cohort |
| Accuracy | 0.753 | 0.721 |
| AUC | 0.753 | 0.754 |
| Sensitivity | 0.750 | 0.714 |
| Specificity | 0.750 | 0.724 |

AUC, area under receiver operating characteristics curve.

outcome predictors in cervical cancer,[29] which were not studied in our work.

In summary, we demonstrated that there is an association between the radiomic signature and LN status in early-stage cervical cancer. This association may lead to a clinical impact on the individualization of cancer therapies.

## Acknowledgments

Contract grant sponsor: National Natural Science Foundation of China; contract grant numbers: 81771924, 81501616, 81671851, 81527805, 81601492, Contract grant sponsor: National Key R&D Program of China; contract grant numbers: 2017YFA0205200, 2017YFC1308700, 2017YFC1308701, 2017YFC1309100; Contract grant sponsor: Science and Technology Service Network Initiative of the Chinese Academy of Sciences; contract grant number: KFJ-SW-STS-160; Contract grant sponsor: Instrument Developing Project of the Chinese Academy of Sciences; contract grant number: YZ201502; Contract grant sponsor: Beijing Municipal Science and Technology Commission; contract grant number: Z161100002616022; Contract grant sponsor: Youth Innovation Promotion Association CAS, and Special Fund for Research in the Public Interest of China; contract grant number: 201402020

## References

1. Siegel RL, Miller KD, Jemal A. Cancer statistics, 2015. CA Cancer J Clin 2015;65:5–29.
2. Koh WJ, Aburustum NR, Bean S, et al. Uterine neoplasms, v. 1. 2018, NCCN Clinical Practice Guidelines in Oncology. J Natl Compreh Cancer Network 2018;16:170–199.
3. Yuan C, Wang P, Lai C, et al. Recurrence and survival analyses of 1,115 cervical cancer patients treated with radical hysterectomy. Gynecol Obstet Invest 1999;47:127–132.
4. Biewenga P, Van dVJ, Mol BW, et al. Prognostic model for survival in patients with early stage cervical cancer. Cancer 2011;117:768–776.
5. SEER Data: Surveillance, Epidemiology and End Results. (Accessed 2015 Sept 19.) Available from URL: http://seer.cancer.gov/statfacts/html/cervix.html
6. Kupets R, Covens A. Is the International Federation of Gynecology and Obstetrics staging system for cervical carcinoma able to predict survival in patients with cervical carcinoma?. An assessment of clinimetric properties. Cancer 2001;92:796–804.
7. Plante M, Renaud MC, Têtu B, et al. Laparoscopic sentinel node mapping in early-stage cervical cancer. Gynecol Oncol 2003;91:494–503.
8. Franchi M, Ghezzi F, Riva C, Miglierina M, Buttarelli M, Bolis P. Postoperative complications after pelvic lymphadenectomy for the surgical staging of endometrial cancer. J Surg Oncol 2001;78:232–237.
9. Levenback C, Coleman RL, Burke TW, et al. Lymphatic mapping and sentinel node identification in patients with cervix cancer undergoing radical hysterectomy and pelvic lymphadenectomy. J Clin Oncol 2002;20:688–693.
10. Matsuura Y, Kawagoe T, Toki N, Tanaka M, Kashimura M. Long-standing complications after treatment for cancer of the uterine cervix—clinical significance of medical examination at 5 years after treatment. Int J Gynecol Cancer 2010;16:294–297.
11. King AD, Tse GM, Ahuja AT, et al. Necrosis in metastatic neck nodes: diagnostic accuracy of CT, MR imaging, and US. Radiology 2004;230:720–726.
12. Williams AD, Cousins C, Soutter WP, et al. Detection of pelvic lymph node metastases in gynecologic malignancy: a comparison of CT, MR imaging, and positron emission tomography. AJR Am J Roentgenol 2001;177:343–348.
13. Lambin P, Leijenaar R, Deist TM, et al. Radiomics: the bridge between medical imaging and personalized medicine. Nat Rev Clin Oncol 2017;14:739–762.
14. Virendra K, Yuhua G, Satrajit B, et al. Radiomics: the process and the challenges. Magn Reson Imaging 2012;30:1234–1248.
15. Gillies RJ, Kinahan PE, Hricak H. Radiomics: Images are more than pictures, they are data. Radiology 2016;278:563.
16. Brown G, Pocock A, Zhao MJ, Luján M. Conditional likelihood maximisation: a unifying framework for information theoretic feature selection. J Mach Learn Res 2012;13:27–66.
17. Wu S, Zheng J, Li Y, et al. A radiomics nomogram for the preoperative prediction of lymph node metastasis in bladder cancer. Clin Cancer Res 2017;23:6904–6911.
18. Huang YQ, Liang CH, He L, et al. Development and validation of a radiomics nomogram for preoperative prediction of lymph node metastasis in colorectal cancer. Sci Found China 2016;34:2157.
19. Limkin EJ, Sun R, Dercle L, et al. Promises and challenges for the implementation of computational medical imaging (radiomics) in oncology. Ann Oncol 2017;28:1191.
20. Lambin P, Leijenaar R, Deist TM, et al. Radiomics: the bridge between medical imaging and personalized medicine. Nat Rev Clin Oncol 2017;14:749–762.
21. Bourgioti C, Chatoupis K, Moulopoulos LA. Current imaging strategies for the evaluation of uterine cervical cancer. World J Radiol 2016;8:342.
22. Delgado G, Bundy BN Jr, Stehman FB, et al. A prospective surgical pathological study of stage I squamous carcinoma of the cervix: a Gynecologic Oncology Group Study. Gynecol Oncol 1989;32:397–397.
23. Look KY, Brunetto VL, Clarke-Pearson DL, et al. An analysis of cell type in patients with surgically staged stage IB carcinoma of the cervix: a Gynecologic Oncology Group study. Gynecol Oncol 1996;63:304–311.
24. Cormier B, Diaz JP, Shih K, et al. Establishing a sentinel lymph node mapping algorithm for the treatment of early cervical cancer. Gynecol Oncol 2011;122:275–280.
25. Chen YB, Liao J, Xie R, Chen GL, Chen G. Discrimination of metastatic from hyperplastic pelvic lymph nodes in patients with cervical cancer by diffusion-weighted magnetic resonance imaging. Abdom Imaging 2011;36:102–109.
26. Patel S, Liyanage SH, Sahdev A, Rockall AG, Reznek RH. Imaging of endometrial and cervical cancer. Insights Imaging 2010;1:309–328.
27. Sala E, Wakely S, Senior E, Lomas D. MRI of malignant neoplasms of the uterine corpus and cervix. AJR Am J Roentgenol 2007;188:1577–1587.
28. Cai HB, Ding XH, Zhou YF, Lie DM. Risk factors for cervical cancer in China: a case-control study. Eur J Gynaecol Oncol 2008;29:72–75.
29. Jeanny K, Keun-Yong E, Ah KI, et al. Prognostic value of log odds of positive lymph nodes after radical surgery followed by adjuvant treatment in high-risk cervical cancer. Cancer Res Treat 2016;48:632–640.